2nd International Symposium Robotics and
Manufacturing Research Education and Applications
November 16 - 18, 1988, Albuquerque, NM, USA

COMPLIANT MOTION CONTROL OF A STATICALLY BALANCED DIRECT DRIVE ROBOT

H. Kazerooni and S. Kim

The Productivity Center and the Mechanical Engineering Department
University of Minnesota
Minneapolis, MN 55455

ABSTRACT

A practical architecture, using a four-bar-linkage, is considered for the University of Minnesota direct drive robot [8]. This statically-balanced direct drive robot has been constructed for stability analysis of the robot in constrained manipulation [5 - 7]. As a result of the elimination of the gravity forces (without any counter weights), smaller actuators and consequently smaller amplifiers were chosen. The motors yield acceleration of 5g at the robot end point without overheating. High torque, low speed, brush-less AC synchronous motors are used to power the robot. Graphite-epoxy composite material is used for the construction of the robot links. A 4-node parallel processor has been used to control the robot. A compliant motion control method has been derived and experimentally verified to guarantee stable constrained maneuvers for the robot. As a part of the research work, a general criterion has been derived to guarantee the stability of robot manipulators in constrained maneuvers.

INTRODUCTION

The University of Minnesota robot is statically balanced and uses a four bar link mechanism to compensate for some of the drawbacks of serial type [2] and parallelogram type [3] direct drive robots.

Conventional robot manipulators with electric servomotors are driven through speed reducers. Although speed reducers generate large torque, they usually introduce backlash, compliance, cogging, and friction into the systems. Studies on several industrial robots indicate that the powertrain compliance forms over 80% of total arm compliance [10]. Also the friction torque generated by reducer is about 25% of the total required torque in any maneuver [4]. Several attempts have been made to improve the manipulator dynamic behavior. Asada and Kanade [2] designed a serial type direct drive arm in which the actuators were directly coupled to links without any transmission mechanism. The elimination of the transmission mechanism improved the robot performance, however large motors were needed to drive the robot. Asada and Youcef-Toumi [3] studied a direct drive arm with a parallelogram mechanism to eliminate the problems associated with serial type robots. A direct drive arm with a counterweight was designed by Takase et al. [11] in order to eliminate the gravity effect at three major joints. Another direct drive arm, designed by Kuwahara et al. [9] to reduce the effect of gravity using a four bar link for the forearm, and a special spring for the upper arm. The counterweight provides the system balance for all possible positions, however it increases the total inertia of the robot arm. The spring balancing will not perfectly balance the system either.

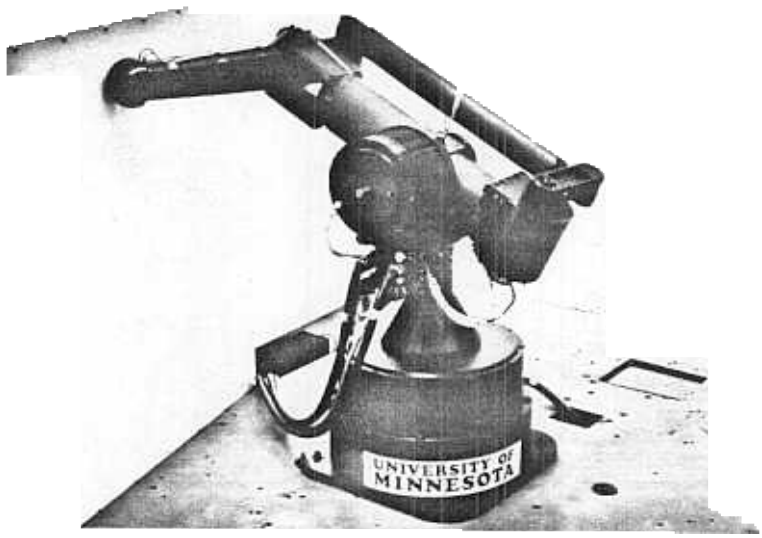

Figure 1: University of Minnesota Direct Drive Arm

In this research, a statically balanced direct drive arm is designed to achieve improved dynamic behavior. As a result of the elimination of the gravity forces (without any counter weights), smaller actuators and consequently smaller amplifiers were chosen. The motors yield acceleration of 5g at the end point without overheating. The control method explained here is general and applies to all industrial and research robot manipulators. We take the time-domain nonlinear approach to arrive at the controller design methodology and its stability condition. The detailed controller design is given in [7]. A summary of the nonlinear modeling and the controller design is given here. In general, manipulation consists of two categories. In the first category, the manipulator end-point is free to move in all directions. In the second, the manipulator end-point interacts mechanically with the environment. Most assembly operations and manufacturing tasks require mechanical interactions with the environment or with the object being manipulated, along with "fast" motion in free and unconstrained space. Therefore the object of the control task on this robot is to develop a control system such that the robot will be capable of "handling" both types of maneuvers without any hardware and software switches.

ARCHITECTURE

Figure 2 shows the schematic diagram of the University of Minnesota direct drive arm. The arm has three degrees of freedom, all of which are articulated drive joints. Motor 1 powers the system about a vertical axis. Motor 2 pitches the entire four-bar-linkage while motor 3 is used to power the four-bar-linkage. Link 2 is directly connected to the shaft of motor 2. The joint angles are represented by θ_1, θ_2, and θ_3. θ_1 represents the rotation of link 1. θ_2 represents the pitch angle of

the four-bar-linkage as shown in figure 3. θ_3 represents the angle between link 2 and link 3. Shown are the conditions under which the gravity terms are eliminated from the dynamic equations.

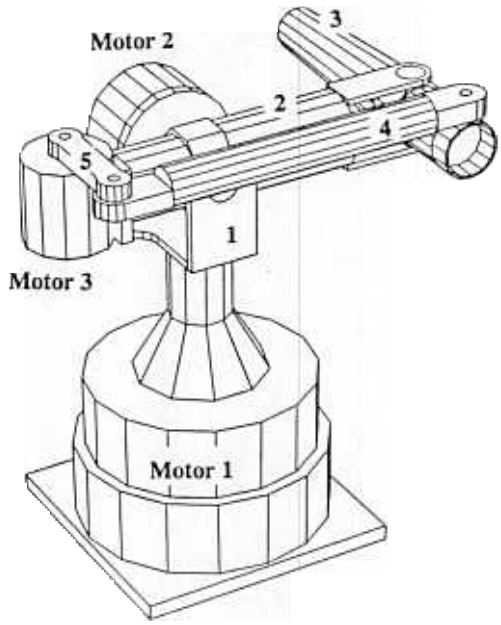

Figure 2: Schematic of University of Minnesota Arm

Figure 3 shows the four-bar-linkage with assigned coordinate frames. By inspection the conditions under which the vector of gravity passes through origin, O, for all possible values of θ_1 and θ_3 are given by equations (1) and (2).

$$(m_3\bar{x}_3 - m_4L_5 - m_5\bar{x}_5) \sin\theta_3 = 0 \tag{1}$$

$$g\,(mt_3 + m_5) - m_2\bar{x}_2 - m_3(L_2 - g) - m_4(\bar{x}_4 - g) - (m_3\bar{x}_3 - m_4L_5 - m_5\bar{x}_5) \cos\theta_3 = 0 \tag{2}$$

where m_i, L_i is the mass and length of each link, $\bar{x}_i$ is the distance of center of mass from the origin of each coordinate frame, mt_3 is the mass of motor 3. Conditions (1) and (2) result in:

$$m_3\bar{x}_3 - m_4L_5 - m_5\bar{x}_5 = 0 \tag{3}$$

$$g(mt_3+m_5)-m_2\bar{x}_2-m_3(L_2-g)-m_4(\bar{x}_4 - g) = 0 \tag{4}$$

If equations (3) and (4) are satisfied, then the center of gravity of the four-bar-linkage passes through point O for all the possible configurations of the arm. Note that the gravity force still passes through O even if the plane of the four-bar-linkage is tilted by motor 2 for all values of θ_2. The dynamic and kinematic analysis are given in reference [8].

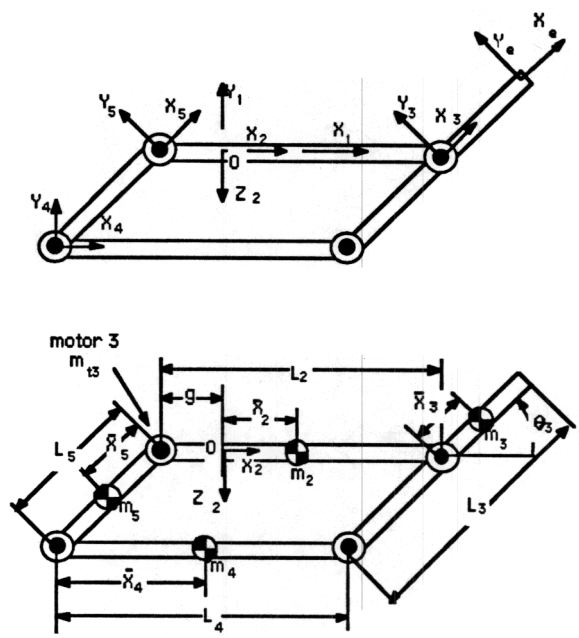

Figure 3: Four bar link mechanism

HARDWARE

A schematic of the system hardware is shown in figure 4. An IBM AT microcomputer which is hosting a 4-node parallel processor is used as the main controller of this robot. The parallel processor has four nodes and a PC/AT bus interface. Each node is an independent 32-bit processor with local memory and communication links to the other nodes in the system. A high speed AD/DA converter has been used for reading the velocity signals and sending analog command signals to the servo controller unit. A parallel IO board (D/D converter) between the servo controller unit and the computer allows for reading the R/D (Resolver to Digital) converter.

The servo controller unit produces three phase, Pulse Width Modulated (PWM), sinusoidal currents for the power amplifier. The servo controller unit contains an interpolator, R/D converter and a communication interface for the computer. The servo controller unit can be operated in either a closed loop velocity or current (torque) control mode (the current control is used). A PWM power amplifier, which provides up to 47 Amperes of drive current from a 325 volt power supply, is used to power the motors. The main DC bus power is derived by full-wave rectifying the three phase 230VAC incoming power. This yields a DC bus voltage of 325VDC. The motors used in this robot are neodymium (NdFeB) magnet AC brushless synchronous motor. Due to the high magnetic field strength (maximum energy products: 35 MGOe) of the rare earth NdFeB magnets, the motors have high torque to weight ratio. Pancake type resolvers are used as position and velocity sensors. The peak torque of motor 1 is 118 Nm, while the peak torques of motors 2 and 3 are 78 and 58 Nm respectively.

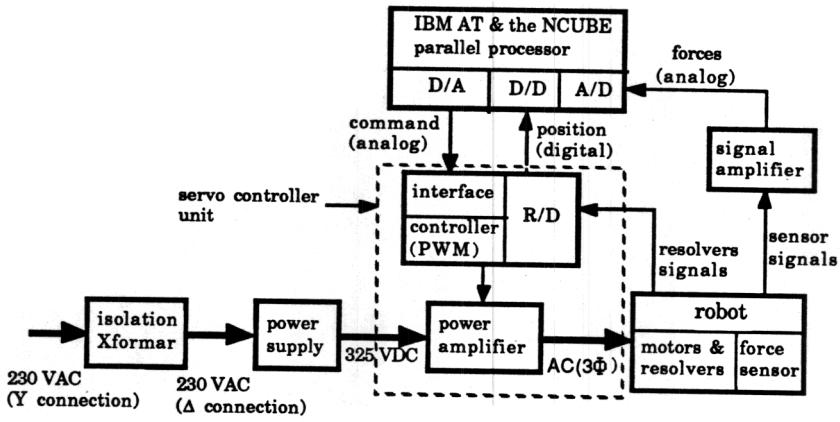

Figure 4: The control hardware for Minnesota Robot

ROBUST, NONLINEAR IMPEDANCE CONTROL

The design objective is to provide a stabilizing dynamic compensator for the robot manipulator such that the following design specifications are satisfied.
(1) The robot end-point follows an input-command vector, r, when the robot manipulator is free to move.
(2) The contact force, f, is a function of the input command vector, r, when the robot is in contact with the environment.

The first design specification allows for free manipulation when the robot is not constrained. If the robot encounters the environment, then according to the second design specification, the contact force will be a function of the input command vector. Thus, the system will not have a large and uncontrollable contact force. Note that r is an input command vector that is used for both unconstrained and constrained maneuverings. The end-point of the robot will follow r when the robot is unconstrained, while the contact force will be a function of r (preferably a linear function for some bounded frequency range of r) when the robot is constrained.

Note that the above notation does not imply a force control technique [13]. We are looking for a controller that guarantees the tracking of the input-command vector when the robot is not constrained, as well as the relation of the contact-force vector with the same input-command vector when the robot encounters an unknown environment.

The general form of the non-linear dynamic equations of a robot manipulator with positioning controller is given by two non-linear vector functions G and S in equation (5).

$$y = G(e) + S(d) \tag{5}$$

where:

- d = n x1 vector of the external force on the robot end-point
- e = n x 1 input trajectory vector
- G = robot dynamics with positioning controller
- S = robot manipulator sensitiveness
- y = n x 1 vector of the robot end-point position

e is the n x 1 input trajectory vector that the robot manipulator accepts via its positioning controller. The fact that most manipulators have some kind of positioning controller is the motivation behind our approach. Also, a number of methodologies exist for the development of the robust positioning controllers for

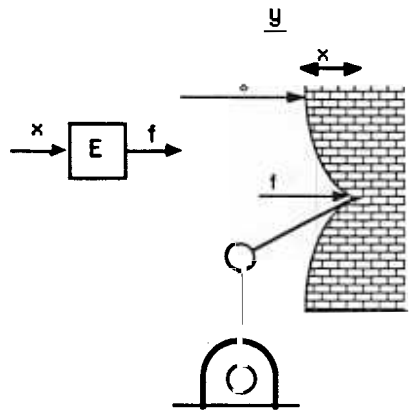
y
x
x
E
f
f

contact with the environment. The lower feedback loop is the controlled feedback loop.

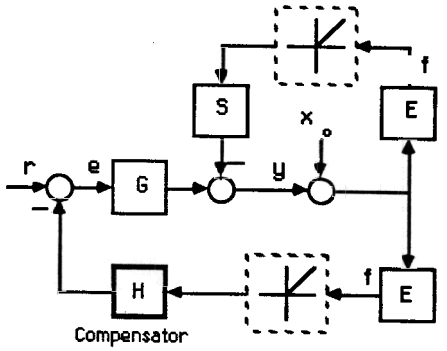

Figure 6: Closed-loop system

If the robot and the environment are not in contact, then the dynamic behavior of the system reduces to y = G(r). When the robot and the environment are in contact, then the value of the contact force and the end-point position of robot are given by f and y where the following equations are true:

$$y = G(e) - S(f) \tag{7}$$

$$f = E(x) \tag{8}$$

$$e = r - H(f) \tag{9}$$

We choose a class of compensators, H, to control the contact force with the input command, r. This controller must also guarantee the stability of the closed-loop system shown in Figure 6. The input command vector, r, is used differently for the two categories of maneuverings; as an input trajectory command in unconstrained space and as a command to control of force in constrained space. We do not command any set-point for force as we do in admittance control. This method is called Impedance Control because it accepts a position vector as input and it reflects a force vector as output. There is no hardware or software switch in the control system when the robot travels from unconstrained space to constrained space. The feedback loop on the contact force closes naturally when the robot encounters the environment. V is introduced to represent the forward loop mapping from e to f. To guarantee the stability of the closed loop system, the L_p-norm of H must be less than the reciprocal of the "magnitude" (in the L_p-sense) of the mapping V in Figure 7.

$$\| H \|_p \leq \frac{\| e \|_p}{\| V(e) \|_p} \tag{10}$$

where $\| \cdot \|_p$ represents the P-norm of a function.

A similar result has been derived for linear case (invariant inertia robot) using Nyquist stability Criteria in [7].

$$\sigma_{max}[H] \leq \frac{}{\sigma_{max}[E(SE + I_n)^{-1}G]} \quad \text{for all } \omega \in (0,\infty) \tag{11}$$

where σ_{max} indicates the maximum singular value[1]. The stability bound automatically leads to selection of the class of compensators, H. For more details on stability bound, see reference [7]

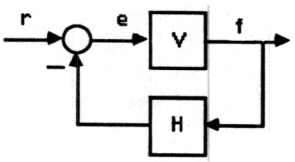

Figure 7: Manipulator and the environment with force feedback compensator, H (simplified version of Figure 6)

EXPERIMENTAL RESULTS

In order to examine the behavior of the proposed compliant motion controller, experiments have been conducted. Our goals were to examine the feasibility of the controller with respect to interaction between force and position control stability. A three dimensional force sensor (Kistler, type 9251 A) is mounted at the wrist of the manipulator to measure the forces at the wrist coordinate. The end effector has a hemispherical shape (radius : 45.7 mm; weight : 0.4 kg) made of aluminium alloy 2024 T6 to avoid moment force applied to the force sensor. The surface of the end effector was hard coated to reduce friction and increase abrasion resistance. An aluminium alloy wall is used as an environment and is located 0.51 m from the origin of the robot global coordinate as shown in Figure 8. The reference trajectory in the experiment is an arc (Radius = 0.54 m). The linear speed of the end effector is 0.42 m/sec.

Considerable high frequency noise in the force sensor output was observed in excess of 200 Hz. To eliminate this effect, the signal from the force sensor was passed through a low pass filter. If the sampled signal has frequency components higher than sampling frequency, aliasing can produce unwanted noise on the sensed force. To reduce aliasing noise, low pass filters, which have cut off frequencies of 70 Hz, were used to cut off at less than one half the sampling frequency. The sampling rate of the force sensor is 147 Hz (6.8 msecs).

All feedback gains were chosen empirically to provide stable, responsive, accurate behavior. No formal optimality criteria was employed. Note that no corrections were made for acceleration forces on the wrist mass.

Figure 9 shows the actual performance of the compliant motion controller on the aluminium wall surface for a given constant speed. The compensator used is the first order, the gain used is 0.005 for the normal direction to the wall, and 0 for the tangential direction, the time constant of the compensator was 0.05. Figure 9 shows the contact force against time when the force feedback is applied. Upon contacting the wall, the end effector slides along a chord of the radius defined by the surface of the wall. At the moment of contact with the wall there is an impulsive force due to the collision of the end effector with the rigid surface, but immediately afterward the force drops to zero. The apparently random fluctuations are due to noise in the system. The difference between the actual position and desired position results in a contact force determined by the target impedance.

---

[1] The maximum singular value of a matrix A, $\sigma_{max}(A)$ is defined as:

$$\sigma_{max}(A) = \max \frac{|AZ|}{|Z|}$$

where Z is a non-zero vector and |·| denotes the Euclidean norm.

From figure 9, it is clear that the compliant motion control scheme using impedance control method shows good control of the interface force during contact task. Therefore, the robot end-point follows an input-command vector, r, when the robot manipulator is free to move, and the contact force, f, is a function of the input command vector, r, when the robot is in contact with the environment.

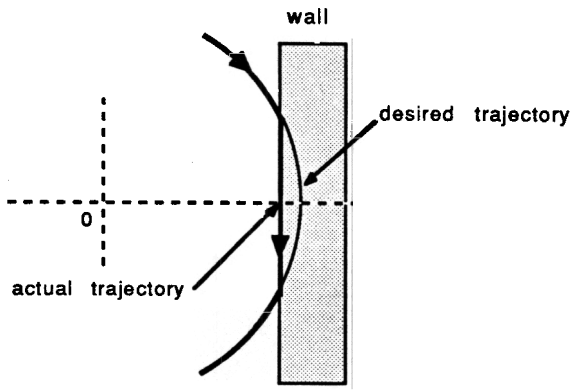

Figure 8: Trajectory of the end effector: actual path is heavy line; velocity is 0.42 m/sec

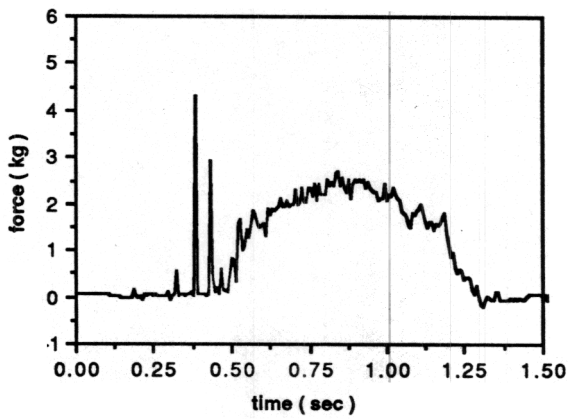

Figure 9: Actual contact force on the aluminium surface vs. time for normal direction with force feedback. The contact force is a function of desired trajectory.

SUMMARY

This paper presents some results of the on-going research project on statically-balanced direct drive arm at the University of Minnesota.The following features characterize this robot:

The statically-balanced mechanism without counter weights allows for selection of smaller actuators. Since in static or quasi-static operations, no load is on the actuators, the overheating of the previous direct drive robots is alleviated. The

robot links are made of graphite-epoxy composite materials to give more structural stiffness and less mass. The high structural stiffness and low mass of the links allow for the wide bandwidth of the control system.

Compliance control has been considered for control of the robot. The stability criterion has been investigated using unstructured models for the dynamic behavior of the robot manipulator and the environment. A compliant motion control method was experimentally verified to guarantee stable constrained maneuvers for the robot. The experimental result clearly demonstrated that the impedance control is a practical strategy for both constrained and unconstrained tasks. Therefore, the robot end-point follows an input-command vector, r, when the robot manipulator is free to move, and the contact force, f, is a function of the input command vector, r, when the robot is in contact with the environment.

REFERENCE

1. An, C. H., Atkeson, C. G., J. D., Hollerbach, J. M., "Experimental Determination of the Effect of Feedforward Control on Trajectory Tracking Errors", *1986 IEEE International Conference on Robotics and Automation,* pp 55 - 60
2. Asada, H., Kanade, T., "Design of Direct Drive Mechanical arms", *ASME Journal of Vibration, Acoustics, Stress, and Reliability in Design,* vol. 105, July 1983, pp. 312 - 316
3. Asada, H. and Youcef-Toumi, K.," Analysis and Design of a Direct Drive Arm with a Five-Bar-Link Parallel Drive Mechanism ", *ASME Journal of Dynamic Systems, Measurement and Control,* vol. 106 No. 3, 1984, pp 225-230.
4. Craig, J. J., "*Introduction to Robotics: Mechanics and Control,* Addison-Wesley, Reading, Mass 1986.
5. Kazerooni, H., Sheridan, T., B., Houpt, P. K., "Fundamentals of Robust Compliant Motion for Robot Manipulators" , *IEEE Journal on Robotics and Automation,* vol. 2, NO. 2, June 1986.
6. Kazerooni, H., Houpt, P. K., Sheridan, T., B., " Design Method for Robust Compliant Motion for Robot Manipulators", *IEEE Journal on Robotics and Automation,* vol. 2, NO. 2, June 1986.
7. Kazerooni, H., Tsay, T. I. "Stability Criteria for Robot Compliant Maneuvers", In *proc. of the IEEE International Conference on Robotics and Automation,* Philadelphia, PA, April, 1988.
8. Kazerooni, H and Kim, S., "Statically-Balanced Direct Drive Robot for Compliance Control Analysis", In Shoureshi, Youcef - Toumi and Kazerooni (eds), *Modeling and Control of Robotic Manipulators and Manufacturing Process, DSC - VOL. 6.* ASME Winter Annual Meeting, Boston, MA., Dec. 1987, pp 193 - 201
9. Kuwahara, H., One, Y., Nikaido, M. and Matsumoto, T., " A Precision Direct Drive Robot Arm", *Proceedings American Control Conference,* 1985, pp 722-727.
10.Rivin, E.I., "Effective Rigidity of Robot Structures: Analysis and Enhancement'", *Proceedings of 85 American Control Conference,* 985, 1985, pp 381-382.
11. Takase, K., Hasegawa, T. and Suehiro, T., "*Design and Control of a Direct Drive Manipulator", Proceedings of the International Symposium on Design and Synthesis,* Tokyo, Japan, July 1984, pp 347-352.
12. Vidyasagar, M., Spong, M. W., "Robust Nonlinear Control of Robot Manipulators", CDC, December, 1985.
13.Whitney, D.E., "Force-Feedback Control of Manipulator Fine Motions", *ASME J. of Dynamic Systems, Measurement, and Control :91-97,* June, 1977.